



## Microstructure and tensile properties of a 14Cr ODS ferritic steel

Qian Zhao<sup>a</sup>, Liming Yu<sup>a</sup>, Yongchang Liu<sup>a,\*</sup>, Yuan Huang<sup>a</sup>, Zongqing Ma<sup>a</sup>, Huijun Li<sup>a</sup>, Jiefeng Wu<sup>b</sup>

<sup>a</sup> State Key Lab of Hydraulic Engineering Simulation and Safety, School of Materials Science & Engineering, Tianjin University, Tianjin 300072, China

<sup>b</sup> Institute of Plasma Physics, Chinese Academy of Sciences, Hefei 230031, China

### ARTICLE INFO

#### Keywords:

Oxide dispersion strengthened steel

Microstructure

Nanoparticle

Tensile property

### ABSTRACT

The excellent mechanical performance of oxide dispersion strengthened (ODS) steels is attributed to the highly dispersed and extremely stable oxide particles with diameters of a few nanometers. Studies were made to determine the microstructure and tensile properties of a 14Cr ODS ferritic steel with the nominal composition of Fe–14Cr–2W–0.3Ti–0.2V–0.07Ta–0.3Y<sub>2</sub>O<sub>3</sub> produced by Hot Isostatic Pressing (HIP) in this work. Through the microstructure investigations, numerous nanoparticles with the average size of 5 nm was found to be located at the grain boundaries and inside the grains, and the average grain size was identified to be approximately 300 nm. The as-HIPed ODS steel proved to have excellent ductility at room temperature by tensile test, which is due to the bimodal structure with uniformly distributed nanoparticles and the addition of vanadium and tantalum.

### 1. Introduction

Development of high performance structural materials for the first wall of the future nuclear reactors is an urgent issue that must be solved in the field of nuclear energy [1,2]. As a kind of advanced structural material, oxidation dispersion strengthened (ODS) steels are selected as the candidate material for the first wall due to the excellent high temperature mechanical properties and good resistance to neutron irradiation, and those remarkable properties are ascribed to the introduced nano-scale oxide particles [1,3–6]. ODS steels are often fabricated by powder metallurgy which consists of mechanical alloying and subsequent consolidation by hot extrusion or hot isostatic pressing [7–9]. The elemental or pre-alloyed powders are mechanically alloyed with Y<sub>2</sub>O<sub>3</sub> powders to obtain stable nanoparticles, and alloying elements such as Al, Zr, and Ti are commonly added in the ODS steels to document the crystal structure, size, distribution, and density of nanoparticles [10–12]. The size of nanoparticles can be effectively reduced by the formation of Y–Ti–O particles resulted from the addition of Ti, and the Y–Ti–O nanoparticles are proved to be stable even at the temperature above 1300 °C [12]. The existence of this kind of nanoparticles can not only hinder the motion of dislocations and grain boundaries but also act as the sinks for the defects produced during neutron irradiation [3].

However, there are still some issues to be settled. The low ductility of the ODS steel is the main problem at present, which may be attributed to the ultrafine grains [13]. As the main mechanical properties of most materials, strength and ductility usually have contrary

relationship. The more difficult it is for the motion of dislocation, the more highly that the strength of material is increased along with the reduction in ductility. In order to balance the strength and ductility, bimodal structure is exploited in steel [14]. The bimodal structure was first obtained in copper by Wang et al. leading to a remarkable improvement of ductility compared to the copper with conventional microstructure [15]. According to the effective application of bimodal structure in copper, Zhao et al. [16] and Mouawad et al. [17] have developed the ODS steels with bimodal structure by blending the gas-atomized powders with mechanical alloyed powders and solidifying those mixed powders, and the ductility of the ODS steels was finally proved to be improved. The combination of uniformly distributed nanoparticles in high density and the bimodal structure exert great influence on the mechanical properties of ODS steels. Investigations on the microstructure, size distribution, and mechanical properties have been performed on the as-mechanical treated and as-heat treated ODS steels [6–11], while no adequate identifications are conducted on the as-consolidated one.

In current paper, samples of the as-consolidated ODS steel without further heat treatment were studied. Matrix of the as-HIPed ODS steel was characterized by X-Ray diffraction. The morphology, crystal structure, and size distributions of nanoparticles, along with the bimodal structure, were identified in the ODS steel. Besides, the tensile test was conducted at room temperature, and the fracture surfaces were investigated via Scanning Electron Microscope. According to the results of tensile test, the high strength was obtained without the loss of ductility.

\* Corresponding author.

E-mail address: [licmtju@163.com](mailto:licmtju@163.com) (Y. Liu).

## 2. Experimental

The pre-alloyed powders (Seamless Steel Tube Plant, Tianjin, China.) with the nominal composition of Fe–14Cr–2W–0.2V–0.07Ta (wt%) were mixed with 0.3 wt% Ti (purity 99.99 wt%) and 0.3 wt%  $Y_2O_3$  (purity 99.99 wt%) powders to give alloy precursor with the desired composition of Fe–14Cr–2W–0.2V–0.07Ta–0.3Ti–0.3 $Y_2O_3$ . The precursor powders were mechanically alloyed by ball milling (QM-3SP4, Nanjing NanDa Instrument Plant, China) for 30 h at 400 rpm with a ball to powder ratio of 15:1 under high purity argon atmosphere. The powder mass of each milling batch was 10g. The consolidation was conducted via Hot Isostatic Pressing (HIP) at 1150 °C for 3 h under a pressure of 150 MPa.

Matrix of the as-HIPed ODS steel were detected by X-Ray Diffraction using Cu K $\alpha$  Radiation. Microstructure of the as-HIPed samples and size, distribution of the oxide particles were observed by Transmission Electron Microscopy (TEM). TEM thin foils were prepared from the 300  $\mu$ m thick slices which were sliced from the as-HIPed sample, and these slices were mechanically thinned down to 50  $\mu$ m and punched into 3 mm diameter discs. The discs were then electropolished in a double jet electropolishing device with a solution of 5% perchloric acid and 95% ethanol at 20 °C. Tensile test was performed on the tensile specimen which possessed a gauge length of 4 mm at room temperature with a nominal strain rate of  $10^{-3} s^{-1}$ . The fracture surfaces of the post-tensile specimen were investigated by Scanning Electron Microscope (SEM).

## 3. Results and discussion

### 3.1. Microstructure

The XRD pattern of the 14Cr ODS steel after consolidation is shown in Fig. 1. As it is observed, only three most intensive peaks are detected, which belongs to the bcc Fe–Cr based matrix existing in the as-HIPed ODS steel and are attributed to (110), (200), and (211) crystal planes respectively. Diffraction peaks of the dispersed phases are absent, which may result from the small size of those dispersoids. Fig. 2 depicts the TEM graphs of the small and large grains in the 14Cr ODS steel. The average size of the small grains in Fig. 2(a) is approximately 200 nm. Fig. 2(b) illustrates the micron-scale large grain which is surrounded by small grains. The average grain size of the ODS steel is approximately 300 nm. Dislocations that were introduced during the mechanical alloying and consolidation process can also be seen in the large grains. Dislocation movement can be hindered by the pinning effect of the nanoparticles, indicating the strong interaction between the nanoparticles and dislocations, which consequently improve the high temperature mechanical properties of the material [6]. The microstructure of the tested specimen is fully ferritic and appears to

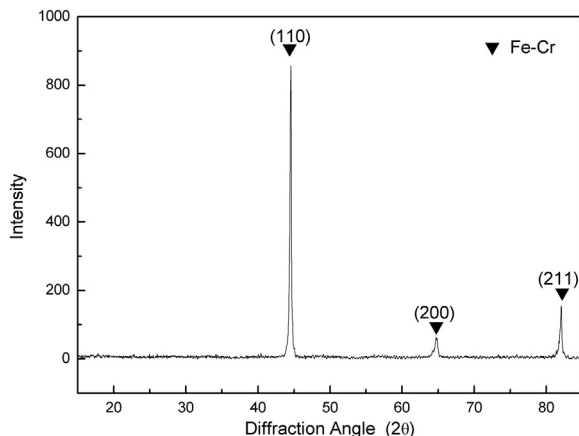


Fig. 1. XRD pattern of the 14 Cr ODS steel after consolidation.

be isotropic. The structure of small and large grains distributing uniformly in the samples is known as bimodal structure. [15]. Differences in grain size can be ascribed to the inhomogeneous milling which leads to the disparity of deformed storage energy in the grains of the milled powders. Deformed energy which was relatively small in the grains of minor deformation was largely stored in the highly deformed grains of the as-milled powders. As the driving force for recrystallization, deformed storage energy with high value can promote the recrystallization process. The grains containing higher deformed storage energy were thus easier to recrystallize, while the ones with smaller deformed storage energy kept stable during the consolidation. In addition, the nanoparticles acting as barriers formed during consolidation, which effectively hindered the growth of the recrystallized grains and efficiently stabilized the unrecrystallized grains. Such a structure with partially recrystallized grains is beneficial for the mechanical properties of the ODS steel. The large grains are beneficial to the ductility due to the active dislocations, whereas the high strength can be attributed to the small grains and the strengthening effect of nanoparticles [16].

### 3.2. Size and distribution of nanoparticles

TEM image of dispersed oxide particles and the HRTEM graph of  $Y_2Ti_2O_7$  particle with the corresponding FFT diagram are illustrated in Fig. 3. As can be seen in Fig. 3(a), the nearly spherical nanoparticles uniformly distribute both inside the grains and on the grain boundaries. The motion of dislocations and grain boundaries can be inhibited by the fine nanoparticles, and as a result the microstructure at high temperature is stabilized, which are conducive to the excellent tensile and creep strength. Moreover, the existence of nanoparticles with high density increases the amounts of interfaces between the nanoparticles and the matrix. This kind of interfaces can act as sinks for irradiation defects such as dislocation loops, voids and helium bubbles, which is beneficial for the high resistance to the irradiation induced hardening and embrittlement [1]. In addition, nanoparticles located on the grain boundaries can effectively retard the movement of grain boundaries and thus restrain the grain growth by the well-known Zener pinning effect during the recovery and recrystallization stage [18]. The nanoparticle with nearly spherical morphology in Fig. 3(b) is identified to be  $Y_2Ti_2O_7$  which is oriented with  $[1\bar{1}0]$  zone axis to the electron beam. The  $Y_2O_3$  particles became fragments and the Ti powders dissolved into the matrix after mechanical milling, which guarantees the formation of nanoscale  $Y_2Ti_2O_7$  particles with high density during the high temperature consolidation process. The addition of Ti has been proved to refine the nanoparticles by the formation of Y–Ti–O particles in the ODS steel [12]. Fig. 4 shows the size distribution of nanoparticles ranging from 1.4 to 12 nm in the 14Cr ODS steel with the average size of approximately 5 nm. According to the histogram, about 98% of the nanoparticles possess the size less than 10 nm, and 61% of them concentrate on the size ranging from 3 to 6 nm. It can be concluded that the Ti and  $Y_2O_3$  particles are equally distributed in the as-milled powders, resulting in the uniform size distribution of Y–Ti–O nanoparticles in the as-HIPed ODS steel.

### 3.3. Tensile properties

Fig. 5 displays the tensile strain–stress curve of the 14Cr ODS steel tested at room temperature. The 14Cr ODS steel possesses the comparative yield and ultimate tensile strength of 710 and 911 MPa respectively at room temperature, comparing with the ODS steel of similar composition [7,19]. But the total elongation has increased by 13% and 35% respectively when compared with the reference Li et al. [7] and Guo et al. [19]. Such results efficiently proved that the bimodal structure of the ODS steel is effective for the improvement of the ductility. The SEM fracture micrographs of tensile samples are illustrated in Fig. 6. Several cracks resulted from the tensile stress

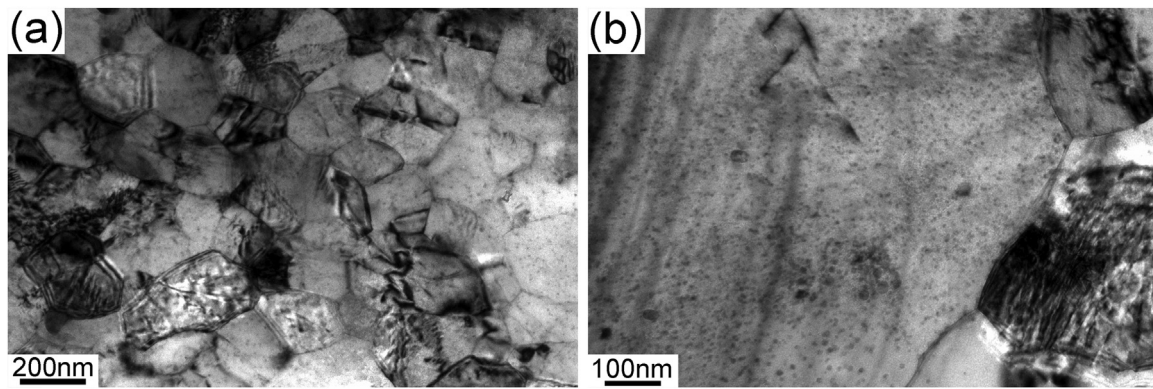


Fig. 2. TEM graphs of the (a) small and (b) large grain in the 14Cr ODS steel.

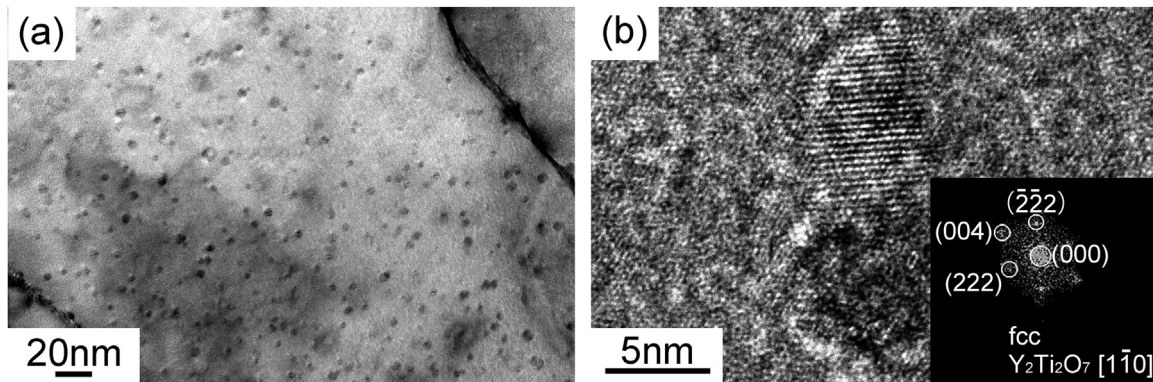


Fig. 3. (a) TEM image of dispersed oxide particles in the 14Cr ODS steel, (b) HRTEM graph of a  $Y_2Ti_2O_7$  particle and the corresponding FFT diagram.

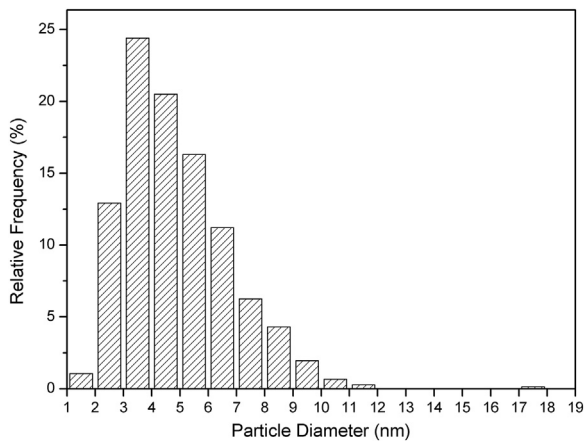


Fig. 4. Size distribution of oxide particles in the 14Cr ODS steel.

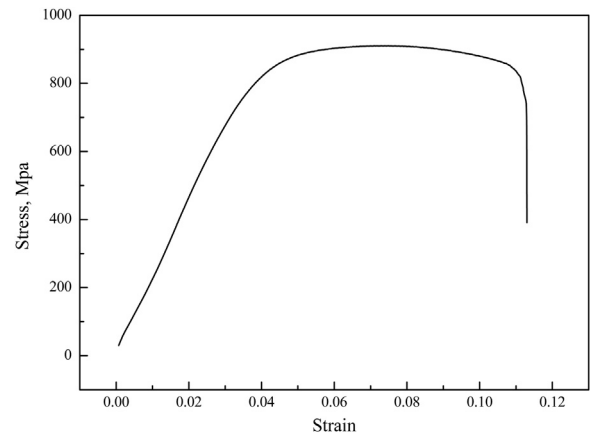


Fig. 5. Tensile strain-stress curve of the 14Cr ODS steel at room temperature.

during the testing can be seen in Fig. 6(a). Besides, both of the cleavage fractures with river patterns and dimpled appearances are shown in the same picture, implying the mixed mode of ductile and brittle fracture. As can be seen from the bottom right of the Fig. 6(a), the cleavage facets with river patterns show the direction of crack propagation, which was nucleated on the grain boundaries and propagated into the interior of the grains, and the formation of cracks are ascribed to the micropores on the grain boundaries. Besides, the defects of micropores, coarse precipitations which combine weakly with the matrix are the favorable sites for the generation of cracks either. The existence of micropores in the fracture surfaces is due to the entrapment of argon during mechanical milling. Part of the entrapped argon would not escape by diffusion along grain boundaries, resulting in the formation of pores during the consolidation process, and these micropores would affect the ductility of the structural materials during tensile test.

Fig. 6(b) demonstrates the deeper dimples in fracture surface at high magnification. The average size of dimples is 580 nm, and the dimple boundaries are very distinctive. The high yield strength, combining with the ductile/brittle mixed fracture mode and the large amount of deep dimples, indicates the excellent ductile properties of the ODS steel when compared to the material with similar composition and fabrication process. The addition of solute elements make contribution to refine the grains, and result in the improvement of strength. According to the investigations by some researchers, tantalum has a positive effect on strength, and the toughness of materials alloyed with tantalum is superior to the materials without tantalum [20]. Moreover, the addition of vanadium also benefits the mechanical properties of structural materials by means of solution strengthening. In another word, both of the bimodal structure and the addition of solute elements promote the improvement of mechanical properties of the ODS steel. The large grains in the bimodal structure are beneficial for the plastic

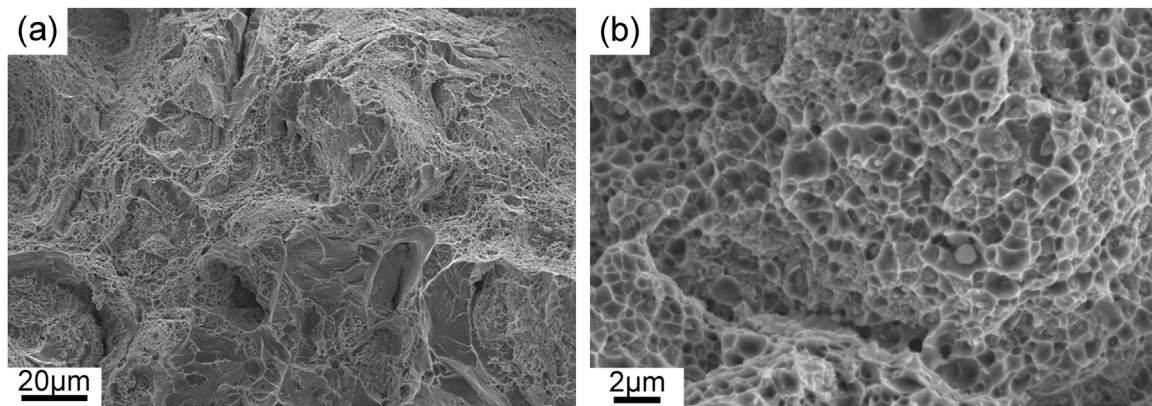


Fig. 6. (a) SEM picture of the typical fracture surface of the 14 Cr ODS steel. (b) Morphologies of the dimple fracture regions at high magnification.

deformation because of the massive dislocations which pill up together and promote the motion of dislocation source in the adjacent grains, and the increase in strength is due to the Hall-Patch relationship between grain size and yield strength.

In general, the microstructure, size and distribution of nanoparticles, and the micropores in the ODS steel have significant influences on the fracture behavior of materials. In other words, tensile properties of the ODS steel depends on the manufacture route and the final heat treatment mode. Even though the densification of the consolidated ODS steel in the current lecture is limited and the micropores exist in the fracture surface, the tensile property is still outstanding because of the bimodal structure and dispersed nanoparticles. When the appropriate heat treatment were performed on the as-consolidated sample, the tensile properties would be further improved.

#### 4. Conclusion

The microstructure and tensile properties of the as-HIPed 14 Cr ODS steel were investigated. The main results have been summarized as follows:

1. Both small and large grains exist in the ODS steel with the size of approximately 200 nm and several micrometers respectively, showing the characterization of bimodal structure that is beneficial for the mechanical properties of structural material by balancing the strength and ductility.
2. The average size of Y-Ti-O nanoparticles in the ODS steel is approximately 5 nm, and the  $Y_2Ti_2O_7$  with fcc structure is identified. The size distribution of nanoparticles is ranging from 1.4 to 12 nm and concentrates on the size ranging from 3 to 6 nm.
3. The yield and tensile strength of the ODS steel are 1045 and 1150 MPa respectively, and the fracture surfaces present a brittle/ductile mixed fracture mode other than quasi-brittle fracture obtained in other research. The improvement on the ductility of the ODS steel is due to the bimodal structure and uniformly distributed Y-Ti-O nanoparticles.

#### Acknowledgements

The authors are grateful to the International Thermonuclear Experimental Reactor (ITER) Program Special Project (No. 2014GB125006 and 2015GB107003), China National Funds for Distinguished Young Scientists (No. 51325401), the National Nature Science Foundation of China (No. 51474155), and Natural Science Foundation of Tianjin City (No. 13JCZDJC31900 and No. 14JCZDJC38700) for grant and financial support.

#### References

- [1] R.L. Klueh, Elevated temperature ferritic and martensitic steels and their application to future nuclear reactors, *Int. Mater. Rev.* 50 (2005) 287–310.
- [2] X. Zhou, C. Liu, L. Yu, Y. Liu, H. Li, Phase transformation behavior and microstructural control of high-cr martensitic/ferritic heat-resistant steels for power and nuclear plants: a review, *J. Mater. Sci. Technol.* 31 (2015) 235–242.
- [3] D.T. Hoelzer, J. Bentley, M.A. Sokolov, M.K. Miller, G.R. Odette, M.J. Alinger, Influence of particle dispersions on the high-temperature strength of ferritic alloys, *J. Nucl. Mater.* 367–370 (2007) 166–172.
- [4] Z. Oksiuta, A. Ozieblo, K. Perkowski, M. Osuchowski, M. Lewandowska, Influence of HIP pressure on tensile properties of a 14Cr ODS ferritic steel, *Fusion Eng. Des.* 89 (2014) 137–141.
- [5] A. Paúl, E. Alves, L.C. Alves, C. Marques, R. Lindau, J.A. Odriozola, Microstructural characterization of Eurofer-ODS RAFM steel in the normalized and tempered condition and after thermal aging in simulated fusion conditions, *Fusion Eng. Des.* 75–79 (2005) 1061–1065.
- [6] M. Saber, W. Xu, L. Li, Y. Zhu, C.C. Koch, R.O. Scattergood, Size effect of primary  $Y_2O_3$  additions on the characteristics of the nanostructured ferritic ODS alloys: Comparing as-milled and as-milled/annealed alloys using S/TEM, *J. Nucl. Mater.* 452 (2014) 223–229.
- [7] Y. Li, J. Shen, F. Li, H. Yang, S. Kano, Y. Matsukawa, Y. Satoh, H. Fu, H. Abe, T. Muroga, Effects of fabrication processing on the microstructure and mechanical properties of oxide dispersion strengthening steels, *Mater. Sci. Eng.: A* 654 (2016) 203–212.
- [8] P. Olier, J. Malaplate, M.H. Mathon, D. Nunes, D. Hamon, L. Toulabi, Y. de Carlan, L. Chaffron, Chemical and microstructural evolution on ODS Fe–14CrWTi steel during manufacturing stages, *J. Nucl. Mater.* 428 (2012) 40–46.
- [9] R. Lindau, A. Möslang, M. Schirra, P. Schlossmacher, M. Klimentov, Mechanical and microstructural properties of a HIPped RAFM ODS-steel, *J. Nucl. Mater.* 307 (2002) 769–772.
- [10] G. Zhang, Z. Zhou, K. Mo, Y. Miao, S. Li, X. Liu, M. Wang, J.-S. Park, J. Almer, J.F. Stubbins, The comparison of microstructures and mechanical properties between 14Cr-Al and 14Cr-Ti ferritic ODS alloys, *Mater. Des.* 98 (2016) 61–67.
- [11] R. Gao, L.L. Xia, T. Zhang, X.P. Wang, Q.F. Fang, C.S. Liu, Oxidation resistance in LBE and air and tensile properties of ODS ferritic steels containing Al/Zr elements, *J. Nucl. Mater.* 455 (2014) 407–411.
- [12] M. Ratti, D. Leuvre, M.H. Mathon, Y. de Carlan, Influence of titanium on nano-cluster (Y, Ti, O) stability in ODS ferritic materials, *J. Nucl. Mater.* 386–388 (2009) 540–543.
- [13] H. Mughrabi, H.W. Höppel, M. Kautz, Fatigue and microstructure of ultrafine-grained metals produced by severe plastic deformation, *Scr. Mater.* 51 (2004) 807–812.
- [14] B. Srinivasarao, K. Oh-ishi, T. Ohkubo, K. Hono, Bimodally grained high-strength Fe fabricated by mechanical alloying and spark plasma sintering, *Acta Mater.* 57 (2009) 3277–3286.
- [15] Y. Wang, M. Chen, F. Zhou, E. Ma, High tensile ductility in a nanostructured metal, *Nature* 419 (2002) 912–915.
- [16] D. Zhao, Y. Liu, F. Liu, Y. Wen, L. Zhang, Y. Dou, ODS ferritic steel engineered with bimodal grain size for high strength and ductility, *Mater. Lett.* 65 (2011) 1672–1674.
- [17] B. Mouawad, X. Boulnat, D. Fabrègue, M. Perez, Y. de Carlan, Tailoring the microstructure and the mechanical properties of ultrafine grained high strength ferritic steels by powder metallurgy, *J. Nucl. Mater.* 465 (2015) 54–62.
- [18] W. Sha, H.K.D.K.H. Bhadeshia, Characterization of mechanically alloyed oxide dispersion-strengthened nickel-base superalloy MA760, *Metall. Mater. Trans. A* 25 (1994) 705–714.
- [19] L. Guo, C. Jia, B. Hu, H. Li, Microstructure and mechanical properties of an oxide dispersion strengthened ferritic steel by a new fabrication route, *Mater. Sci. Eng.: A* 527 (2010) 5220–5224.
- [20] R.L. Klueh, D.J. Alexander, M.A. Sokolov, Effect of chromium, tungsten, tantalum, and boron on mechanical properties of 5–9Cr–WVTaB steels, *J. Nucl. Mater.* 304 (2002) 139–152.